LAWRENCE
LIVERMORE
NATIONAL
LABORATORY

LLNL-JRNL-647814

High-Density Carbon Ablator Experiments on the National Ignition Facility

A. J. MacKinnon, N. Meezan, J. S. Ross, S. Le Pape, L. Berzak-Hopkins, L. Divol, D. Ho, J. Milovich, A. Pak, J. Ralph, T. Doeppner, C. Thomas, R. Tommasini, S. Haan, A. G. MacPhee, J. McNaney, J. Caggiano, R. Hatarik, R. Bionta, T. Ma, B. Spears, R. Rygg, R. Benedetti, R. Town, D. Bradley, E. Dewald, D. Fittinghof, O. Jones, H. Robey, J. D. Moody, S. Khan, D. A. Callahan, A. Hamza, J. Biener, P. Celliers, G. Collins, E. Storm, W. Hsing, O. Landen, J. L. Atherton, J. D. Lindl, M. J. Edwards, A. Zylstra, M. Rosenberg, H. Rinderknecht, M. Gatu-Johnson, J. Frenje, R. Petrasso, G. Grim, N. Guler, F. Merrill, R. Olson, J. D. Kilkenny, A. Nikroo, K. Moreno, D. E. Hoover, C. Wild, E. Werner

December 17, 2013

Physics of Plasmas

Disclaimer

High-Density Carbon Ablator Experiments on the National Ignition Facility

A. J. MacKinnon*, N. Meezan, J. S. Ross, S. Le Pape, L. Berzak- Hopkins, L. Divol, D. Ho, J. Milovich, A. Pak, J. Ralph, T. Doeppner, C. Thomas, R. Tommasini, S. Haan, A. G. MacPhee, J. McNaney, J. Caggiano, R. Hatarik, R. Bionta, T. Ma, B. Spears, R. Rygg, R. Benedetti, R. Town, D. Bradley, E. Dewald, D. Fittinghof, O. Jones, H. Robey, J. Moody, S. Khan, D. A. Callahan, A. Hamza, J. Biener, P. Celliers, G. Collins, E. Storm, W. Hsing, O. Landen, J.L. Atherton, J. D. Lindl, M. J. Edwards

Lawrence Livermore National Laboratory, P.O. Box 808, Livermore, CA 94551-0808

A. Zylstra, M.Rosenberg, H. Rinderknecht, M. Gatu-Johnson, J. Frenje, R. Petrasso

Plasma Science and Fusion Center, Massachusetts Institute of Technology, Cambridge, MA 02139

G. Grim, N. Guler, F. Merrill, R. Olson

Los Alamos National Laboratory, Los Alamos, NM 87545

J. D. Kilkenny, A. Nikroo, K. Moreno, and D. E. Hoover

General Atomics, P.O. Box 85608, San Diego, CA 93286-5608

C. Wild, E. Werner

Diamond Materials GMBH, Germany

Abstract:

High Density Carbon (HDC) is a leading candidate as an ablator material for Inertial Confinement Fusion ICF capsules in x-ray (indirect) drive implosions. HDC has a higher density (3.5 g/cc) than plastic (CH , 1g/cc), which results in a thinner ablator with a larger inner radius for a given capsule scale. This leads to higher x-ray absorption and shorter laser pulses compared to equivalent CH designs. This paper will describe a series of experiments carried out to examine the feasibility of using HDC as an ablator using both gas filled hohlraums and lower density, near vacuum hohlraums. These experiments have shown that DD and DT gas filled HDC capsules

driven by a hohlraum filled with 1.2mg/cc He gas, produce neutron yields a factor of 2x higher than equivalent CH implosions, representing better than 50% Yield-over-Clean (YoC). In a near vacuum hohlraum (He = 0.03mg/cc) with 98% laser-to-hohlraum coupling, such a DD gas-filled capsule performed near 1D expectations. A cryogenic layered implosion version was consistent with a fuel velocity = 430 ±50km/s with no observed ablator mixing into the hot spot.

PACS numbers: 52.57Fg,28.52Cx,52.57Bc

*mackinnon2@llnl.gov

I. INTRODUCTION

In the inertial confinement fusion (ICF) hot-spot ignition scheme, kinetic energy from an imploding spherical pusher is converted upon stagnation to internal energy in the fusion fuel hot spot [1]. At the National Ignition Facility (NIF) [2], this is achieved via the indirect-drive method. The fusion capsule consists of a spherical shell of cryogenic deuterium-tritium (DT) fuel surrounded by the ablator. Laser power deposited inside a gold hohlraum is converted to soft x-rays that impinge on the ablator. The ablator material absorbs the x-rays and explodes outward, accelerating the shell and fuel layer inward. In order to achieve a sufficiently high hot spot temperature to initiate thermonuclear burn, the maximum velocity of the cryogenic DT fuel pusher must reach Vfuel ~350 km/s [3]. By the end of the acceleration phase, most (≈ 90 %) of the ablator material surrounding the cryogenic fuel layer has been removed.

Theoretically, to provide the most efficient acceleration, nearly all the ablator material should be removed from the capsule during acceleration—the ablation pressure then acts upon the minimum payload mass [4]. Only a very thin ablator layer is needed to protect the fuel from direct x-ray heating at the end of the implosion. Unfortunately, during the implosion's acceleration phase, the ablation front of the imploding shell is unstable to the Rayleigh-Taylor instability. Although the instability is partially stabilized by the ablation process, it is calculated and observed that defects on the capsule surface grow to several hundred times their original size. It is therefore desirable to keep additional mass between the fuel layer

and the ablation front to separate the hotspot from Rayleigh-Taylor growth at the ablation front. On the other hand, increasing the ablator mass of the capsule increases the laser energy and power needed to drive the fuel pusher to the required velocity.

For the baseline NIF ignition capsule design, these two competing design considerations of velocity and remaining ablator mass were balanced using radiation-hydrodynamics simulations. The resultant goal for the capsule is to achieve a fuel velocity V_{fuel} = 370 km/s with M ≥ 0.25 mg of ablator mass remaining at the time of peak velocity, as described in detail by Meezan et al., [5].

To date most of the indirect drive experiments on the NIF have used CH as the ablator material, however other ablators such as pure carbon (diamond or HDC) and beryllium (Be) have properties that could make them more attractive for achieving high performance implosions as discussed in detail by Haan et al., [3]. The higher density of HDC for the same initial outside diameter leads to a thinner initial shell, hence larger initial inside diameter, leading to more pdV work done on a larger fuel and hot spot volume. In addition, the thinner shell leads to less absolute inward motion during shock compression such that for the same initial outside diameter, the ablation front is at larger radius when peak of the drive and acceleration begins. This leads to higher efficiency than either CH or Be as the HDC capsules absorbs more energy due to a larger ablation surface area. The nano-crystalline nature of HDC, with grain size of order 70nm leads to very smooth surfaces, with surface quality much better than (up to factor of 10) than the requirements inferred from simulations [3].

The higher ablator efficiency and superior surface smoothness of HDC makes it an ideal candidate as an ablator for ignition scale capsules on the NIF, however there is an open question regarding the melting of the diamond during the implosion. Solid or partially melted HDC can provide microstructure that seed hydrodynamic instability, ideally HDC should be completely melted to achieve spatially uniform shocks. Complete melting requires shock strength of > 12Mbar [6,7] while the co-existence state requires shock strength around 6Mbar. Recent experiments [8,9] at the Omega facility [REFERENCE] have shown that keeping

diamond in the coexistence regime is sufficient to reduce shock non uniformities to an acceptable level.

This measurement method employs a time-resolved two-dimensional imaging velocity interferometer (VISAR) illuminated by a 2 ps laser pulse, which captures spatial variations in the velocity across the shock front transmitted through the ablator. The measurement is carried out over an 800 um field of view with relative velocity sensitivity $\delta V/V = 10^{-4}$ and over perturbation wavelengths in the range of 3-4 um to 50 um [8]. Data comparing shock uniformity through Be and HDC are shown in fig.1. Here the Omega laser was used to produce a 4.5Mbar shock in planar samples of Be or HDC. Qualitatively it is clear that the shock uniformity is very good with Be (which has acceptable uniformity at this shock strength) but is much less uniform with HDC at this shock pressure as shown in the 2D velocity uniformity ($\delta V/V$ vs space) maps Fig 1(a) and (b) respectively .

A series of experiments (which will be described in detail in a future publication) was carried out to determine a shock strength where acceptable uniformity for HDC could be obtained. The results are summarized in Fig 1 (c), which plots the velocity uniformity spectrum for 2 shock strengths in HDC compared to Be. An increase in the shock strength to 8Mbar partially melted the HDC leading to a dramatically improved the shock uniformity. From these data it was determined that in order to maintain acceptable shock velocity uniformity the first shock strength > 6Mbar for all NIF HDC implosion designs. All the pulse shapes described in his paper meet this requirement.

The remainder of this paper is divided into sections: Section II will describe the trade-off between instability growth and the fuel adiabat that determined the current pulse shapes used for HDC experiments on the NIF. Section III will describe the experimental setup. Section IV will describe implosion experiments using low adiabat (α = 1.5) 10ns duration laser pulses to drive HDC capsules in conventional gas filled hohlraums [10-13]. Section V will describe high adiabat (α = 3.5) implosion experiments using near vacuum hohlraums for HDC capsules. Section VI will present conclusions and future directions.

II. DESIGN CONSTRAINTS FOR HDC ABLATORS

The most important goals of the HDC campaign on NIF were to determine if there were any fundamental obstacles to obtaining high performing implosions with HDC and also to develop a strategy to approach ignition conditions by starting with a relatively high adiabat and then reducing the adiabat to approach ignition relevant conditions. Here the fuel adiabat, α , is defined as pressure at a given density divided by the Fermi degenerate pressure at that density [3]. Implosions with low adiabat ($\alpha \sim 1.5$) pulseshapes can achieve high compression and fuel density but are more vulnerable to HI, which can adversely affect performance. High adiabat ($\alpha \sim 2$-3.5) pulseshapes cannot achieve high fuel densities and may not be able to reach ignition conditions, however they provide a platform to examine implosion performance while minimizing the effects of HI. By modifying the laser pulseshape we can then gradually reduce α and examine the trade-off between compressibility and HI.

A. Models: Hydrodynamics simulations

The HDC design was developed through a combination of 1 and 2D Radiation Hydrodynamics models. Most of these studies are carried out using Hydra, which is a 3D multi-physics radiation-hydrodynamics code that attempts to include all of the physics needed to model ICF experiments [14]. Two kinds of calculations are described in this paper. 1D capsule only simulations are used to generate a suitable x-ray drive (a frequency-dependent-source or FDS: this is effectively a spectral intensity as a function of time and photon energy $h\nu$) to achieve good 1D performance. 2D integrated (hohlraum + capsule) pre-shot simulations are then used to determine the laser pulse shape required to produce this FDS source and to produce a symmetric implosion. The 2D model described here use the "high-flux model"—electron thermal conduction with a flux-limiter f = 0.15 and the DCA non-LTE atomic physics model—developed after the NIF hohlraum energetics campaign of 2009 [15]. The input laser sources are adjusted to account for backscattered light

and for cross-beam transfer occurring in the hohlraum plasma [10-12]. In addition, the laser source is further degraded to match experimental shock-front and ablator data, as described by Jones et al.[16].

In addition 2 and 3D capsule only simulations are used to evaluate the HI growth factors as a function of ablator material, ablator dopant, x-ray drive (FDS) and measured ablator roughness [3]. Dopants are added to minimize HI growth at the fuel ablator interface by reducing flux of x-rays with $h\upsilon$ >1.8kev that preheat this interface. High levels of preheat lead to a high Atwood number increasing the risk of Rayleigh-Taylor instabilities that mix ablator and cold fuel into the hot spot [3]. Setting the dopant level is essentially a trade-off between HI at the ablation front versus at the fuel ablator interface. High levels of dopant reduce ablative and density gradient stabilization at the ablation front and so increase growth rates there. Depending on the amount of >1.8keV x-rays low dopant levels can allow too much preheat at the fuel ablator interface. To date CH implosions on the NIF have used either Ge or Si dopants [3]. For HDC the current dopant material of choice is tungsten [17] but it is not clear what level of dopant is required. In fact designs with no dopant are predicted to perform well for higher adiabat designs (α >2.5-3.5). Experiments are planned that will investigate this trade-off in detail but near term experiments with HDC have all used undoped capsules.

B Target designs:

A series of 1D and 2D simulations were carried out for HDC designs with increasing number of steps ("shocks") in the x-ray drive. Table 1 summarizes the HDC ablator performance compared to the standard silicon doped CH (Rev 5) design [3] in terms of fuel adiabat, ablator dopant, HI growth factors, fuel velocity, projected 1D yield and stagnated fuel areal density.

From Table.1 it can be seen that the performance of 4 shock, α = 1.5, HDC design is essentially equivalent to the CH 4 shock α = 1.4 design, with roughly twice the higher 1D yield and slightly lower fuel areal density. However the 4-shock HDC design with 0.25% atomic fraction W is more susceptible to HI, as shown by the

ablation front growth factors, which are 1.7x higher than the equivalent CH design. The 3 shock ($\alpha \sim 2$) HDC design (also doped with 0.25% W) has lower HI growth rates with lower compressibility, as shown by the lower fuel areal density. However the 1D performance is comparable to the 4-shock HDC design. The laser pulse duration required to drive the 3 and 4 shock implosions are ~10ns. This is a factor of 2.5 shorter than the equivalent CH 4 shock (22ns) and 50% shorter than the CH 3 shock design (15ns). A direct comparison 4 shock HDC and CH implosions can be made by comparing performance using conventional gas filled hohlraums containing with helium gas with density around 1g/cc [10-13]. The helium gas reduces hohlraum wall motion, allowing a symmetric implosion to be achieved at the expense of increased backscatter and reduced hohlraum efficiency. Using the same gas filled hohlraum platform allows relatively straightforward comparison of ablator performance using a standard and well understood implosion platform, as will be described in section IV.

One can also reduce the ablation front growth factors by more than a factor of 10 by using a higher adiabat (α ~3.7) 2-shock pulse shape and using un-doped HDC capsules. This 2-shock pulse is not an ignition design but it is predicted to produce significant yield in 1D (50kJ yield equivalent to ~2e16 DT neutrons), which would allow valuable insight into implosion performance while minimizing the effect of ablation front HI growth. As discussed above, the lack of dopant increases the risk of HI at the fuel-ablator interface, which can result in mixing of ablator and cold fuel into the hot spot, reducing the hot spot temperature and limiting the neutron yield. The amount of ablator mixing into the hot spot can be estimated from HDC implosions by comparing absolute x-ray and neutron yields using a 1D hotspot model [18,19] to evaluate excess impurity emission.

An even shorter laser pulse of 6ns duration is required to generate the 2-shock x-ray drive for HDC. This short laser duration allows less time for wall motion and plasma filling and opens up the possibility of using hohlraums with very low levels of gas fill (Near Vacuum Hohlraums = NVH). The advantage with a NVH is that it has reduced backscatter, little or no hot electron generation and improved

hohlraum efficiency [20]. The remaining issue with these types of hohlraums is that though reduced, plasma filling still impedes the propagation of the " inner" laser beams. These beams provide the x-ray drive to the capsule equator and impaired propagation leads to asymmetry and/ or time dependent symmetry swings through the peak of the x-ray drive. Achieving symmetry is the biggest challenge to achieving a 1D implosion with these hohlraums. This will be described in Section V. Some promising mitigation schemes using larger shape hohlraums with intermediate levels of hohlraum gas fill are described in section VI.

III. EXPERIMENTAL SETUP

As shown in fig.2, the NIF's 192 beams are arranged into 48 quads, i.e. sets of four beams. These quads are further arranged into inner and outer cones. The two overlapping inner cones consist of 4 quads at 23.5^{o} and 4 quads at 30^{o} each relative to the hohlraum axis of rotation. The outer cones consist of 8 quads at 44.5^{o} and a further 8 quads at 50^{o} each. The inherent inner cone fraction (defined as the inner cone power divided by the total power) of the NIF is thus one third. The total laser energy and peak power delivered by each quad is measured with ±2% and ±3% accuracy, respectively.

The laser power that is backscattered out of the hohlraum is measured on one 30^{o} inner-cone quad and one 50^{o} outer-cone with the full-aperture backscatter station (FABS) and Near Backscatter Imagers (NBI) [21]. These diagnostics measure the energy, power, and spectrum of the stimulated Raman scattered (SRS), and stimulated Brillouin scattered (SBS) light that is reflected directly back towards the final optics. The SRS and SBS are measured with an error of ±20% and ±25%, respectively. The near backscatter imager (NBI) measures SRS and SBS light in an f=4 cone around the quad with an error of ±14%. The SRS and SBS are measured with an error of ±30% for the 23.5^{o} degree beam cone. For the 44.5^{o} quads there is not backscatter measurement and it is assumed to have the same backscatter as the 50^{o} beam cone.

To measure the hot electrons, which can affect the ICF implosion, a filter-fluorescer array, FFLEX, [22] measures the hard x rays (>20keV). From the hard x-

ray spectrum and models of Bremsstrahlung x-ray emission due to electron scattering, the hot electron spectrum can be determined. The FFLEX has eight time integrated channels covering a range from 20 to 80 keV and two high energy time resolved channels with the energy range of 100-220 keV.

The principal x-ray drive diagnostic, Dante [23-26] is an absolutely calibrated, time-resolved 18-channel x-ray diode array that measures the x-ray flux and spectrum from 50 eV to 20 keV emitted through the LEH at an angle of 37° to the hohlraum axis. The spectrometer uses a series of K- and L- edge filters to measure the soft x-ray flux in given bands, which can be unfolded to characterize the soft x-ray spectrum.

The principal x-ray imaging diagnostics used are x-ray framing cameras, [27] which take multiple time-resolved images of either (a) the self-emission of the imploding capsule (Symcap), (b) 1D backlit image of the imploding shell termed 1D convergent ablation (1DCONA) [28] or (c) a 2D backlit image of the imploding shell (2DCONA) [29]. The 1D and 2DCONA targets have hohlraum windows on either side of the capsule and a backlighter foils chosen to give the optimum contrast to measure the shape and density of the ablator. The symcap targets only have a window on one side of the hohlraum. The x-ray framing cameras used to record self-emission or backlit images have a spatial resolution of ~10 μm and a temporal resolution of 40-80 ps. The shapes of the imploding shell and self-emission obtained from the GXD are both sensitive indicators of the symmetry of the x-ray drive.

In order to carry out cryogenic layered implosions, the shocks must first be accurately synchronized. This is achieved using a Velocity Interferometer System for an Any Reflector (VISAR) diagnostic [30, 31] to measure shock timing in surrogate liquid deuterium filled " keyhole" targets as described in detail in Robey et al., [32]. Lastly implosion performance is characterized using a suite of nuclear diagnostics that measure the neutron spectrum from deuterium (DD) and Deuterium-tritium (DT) filled capsules. These diagnostics, described in detail by Frenje et al., [33], measure the absolute neutron yield, ion temperature, primary and scattered

neutron spectrum, neutron bang time and neutron burn duration. These observables are compared to 1 and 2D simulations of both gas filled and cryo layered experiments to evaluate the quality of these implosions.

C Targets: HDC and CH capsules

The experiments described here used 28um thick gold hohlraums, 5.75 mm in diameter, with two different lengths; 9.4 and 10.1mm, and laser entrance holes of 3.1mm diameter for the 9.4mm hohlraums and 3.73mm for the 10.1mm hohlraums respectively. Fig.2 shows a schematic of the target and viewing angles of the primary diagnostics. All three target types used either a CH or HDC capsule placed in the center of the hohlraum. The hohlraums had two levels of He gas fill: (a) "conventional" gas filled hohlraums with a density of 0.96 and 1.2 mg/cc for the 4-shock CH and HDC experiments (b) a NVH with a density of 0.03mg/cc for the 2-shock experiments.

For these experiments un-doped HDC targets were used with two different thicknesses: (a) 76um thick for 4-shock experiments and (b) 86um thick for 2 shock experiments, as shown in Figure 3. The performance of the 4-shock HDC implosions was compared with similar implosions using standard 4-shock pulseshapes for CH capsules in a conventional gas filled hohlraum. In this case the CH capsule had up to 2 % silicon doping and a 20um CH payload to match the mass of a DT ice layer [27]. The HDC capsules for the 2-shock experiments were ~10um thicker than the 4-shock in order to provide a better match for the higher drive obtained from the more efficient NVH, as described in section V.

The HDC and CH targets described in this paper were filled with equi-molar (50/50) mixtures of either D_2 or DT with gas density varying from 3 to 7 mg/cc depending on the experiment. The major difference between SYMCAPs and CONA platforms is the convergent ablator experiments remove two outer quads for backlighting. In the THD 2DCONA experiment a layer of THD ice, 56um thick was formed on the inside of the capsule and was fielded at 1.5 K below the DT triple point.

IV. Gas filled hohlraum experiments

A four shot mini-campaign was completed using HDC capsules in 3 different target platforms. A "keyhole" target [32] was fielded first with a truncated laser pulse for an initial assessment of backscatter and hohlraum performance and shock timing. Two 1D convergent ablator targets were fielded to measure the in-flight capsule velocity and hot spot shape. The final shot in the mini-campaign was a cryogenic symcap target filled with deuterium and tritium gas to assess nuclear performance. The laser pulse shape is shown in fig.4 and compared with a typical CH pulse shape. A peak power of 360 TW with a total laser energy of 1.3 MJ is delivered by 192 laser beams. The HDC pulse is significantly shorter than the two CH pulses due to the faster first shock transit time $\sim 1/\sqrt{}$(Picket Power x shell density)

This pulse was used to drive a 76um thick HDC 505/50 DT symcap. The measured laser to hohlraum coupling level of 91 ± 2%, compared to 87 ±3% average for gas filled hohlraums driving CH capsules [10-13]. The DT neutron yield of $1.6 \times 10^{15} \pm 3 \times 10^{13}$ over a nuclear burn width of 340 ps at an ion temperature of 2.9 ± 0.1 keV represents the highest gas-filled implosion yield to date. The implosion was fairly symmetric with an x-ray measured average hot spot radius, P0 = 57 ± 4 μm and P2/P0 = 0.19 ± 0.08, as shown in fig.5. Using these measured quantities and a 1D hot spot model [19] the hot spot pressure is inferred to be 32.5 Gbar. These values are in close agreement with post shot simulations, giving YoS (1D) of 70%.

The performance of this symcap compared to an equivalent CH gas filled implosions is also shown in Fig . 5, where the measured DT (or DD yield scaled by factor of 100) yield plotted as a function of laser drive energy. The HDC experiment produced a yield 2x higher than any previous CH gas-filled symcaps, which have a similar convergence ratio.

Although this is a very encouraging result it must be noted that in order to match the 2D simulations drive must be significantly degraded using drive multipliers following the same methodology of Jones [16]. These drive multipliers are very similar to those applied to gas-filled hohlraums driving 4-shock CH

capsules, representing an unexplained 15% loss in peak drive compared to simulations. In addition, although the laser coupling was high at 91± 2%, this still represents significant backscatter. Combining these factors represents an energy loss of ~ 200kJ, which appears to remain a fundamental issue related to the energetics of gas filled hohlraums [10-13]. One possible solution to this issue is to use 2-shock pulses with HDC ablators in near vacuum hohlraums, which have demonstrated low levels of backscatter and high coupling [20].

V. NEAR VACUUM HOHLRAUMS

As discussed in section II the short laser duration of the 2 shock HDC pulse (as shown in fig. 6) allows the possibility that a low gas filled hohlraum can be used to achieve a symmetric implosion with low backscatter and good efficiency. A mini campaign of three shots was used to investigate the performance A keyhole target was again fielded first with a truncated laser pulse for an initial assessment of backscatter and hohlraum performance and shock timing. A gas filled cryogenic symcap target filled with deuterium gas was used to assess symmetry and nuclear performance. Finally the implosion velocity and inflight ablator shape pushing on a THD ice layer was measured using a 2D CONA experiment.

Standard 5.75mm diameter hohlraum targets were used for these experiments (as described in section III), but with a minimal helium gas fill of 0.032 mg/cc, required to provide conduction cooling the capsule. Unlike conventional gas-filled hohlraums, in a NVH there is no transfer of energy between the inner and outer beams at peak power and so the implosion symmetry is set by direct adjustments to cone energies. The lack of hohlraum gas also leads to minimal backscatter losses and very efficient drive as shown in the performance of an 86um thick un-doped HDC capsule filled with 3mg/cc DD gas. Table 2 summarizes the performance of this shot with a comparison with post-shot 1D modeling. As expected the laser to hohlraum coupling was 98% and the implosion (at 10x convergence) achieved a record neutron yield of 2.4e13 for a DD gas-filled implosion. The implosion was symmetric and was well described by post-shot

simulations when the simulated M band (x-rays > 1.8keV) was adjusted to match the experimentally measured value. The x-ray bang-time of 7.8ns was consistent with an extremely high shell velocity of 430km/s.

The excellent performance of the symcap implosion is very promising for HDC but cryogenic ice layers with convergence >20x are a more challenging test of implosion performance. A convergent ablation measurement on a THD ice layer provides information on both the implosion velocity and inflight shell shape close to bang time. In addition measurements of the nuclear performance and absolute x-ray emission allow an estimate of ablator mix into the hot spot [18,19].

A truncated version of the 2-shock pulseshape, with laser energy 1.25MJ, was used to drive an 86um thick HDC ablator with a 56um thick THD ice layer (T(75%):H(23%):D(2%)). The implosion was characterized using 2D backlighting with a 7.8 keV Nickel He–α backlighter onto a gated x-ray detector, as described in section II. The backlighter was driven by 8 beams of NIF timed to observe the shell shape from 350ps to 100ps before bang time as shown in fig. 8. Strong capsule self-emission and low contrast images meant that only the first 3 frames could be analyzed for shape and velocity. The shell was quite round with P2 = 2um at a capsule radius P0 = 200um when the shell velocity reached 375 ± 50km/s. This is consistent with an inferred fuel velocity 400 ± 50km/s, obtained by comparison with Hydra post shot simulations (see Meezan et al., [5] for methodology to extract inferred fuel velocities from CONA shell velocity measurements). The inferred fuel velocity vs ablator remaining mass is shown in fig. 9 for this HDC implosion compared to CH THD layered implosion in a gas-filled hohlraum driven by a 1.6MJ 4-shock laser pulse. Hydra post shot simulations for these two implosions are also shown. These data and simulations illustrate the increased drive of a NVH , which achieves significantly higher velocity and more ablated mass for less laser energy than the CH gas filled hohlraum implosion.

An estimate of the ablator mixing into the hot spot was obtained from measurements of the neutron yield, ion temperature and absolute x-ray emission at 11keV measured by the SPBT detector looking through the lower laser entrance

hole [34]. By comparing the observed x-ray emissivity with that expected from a pure DT plasma one can infer the amount of high Z(carbon) in the hotspot [18,19]. The results for the THD experiment are shown in fig.10 compared to a series of CH DT layered implosions. The HDC THD implosion was consistent with essentially zero hotspot mix (<90ng). This is again a very promising result, confirming low hot spot mix in a high velocity implosion, consistent with low ablation front growth rates and pre-shot simulations that predicted low fuel ablator mix for the x-ray drive and level of M band measured in the experiment.

There is however an issue with hot spot symmetry that prevents this implosion from being truly 1D. Pre and post shot 2D simulations indicated that the inner beam propagation is impaired late in the drive (around 6ns) by hohlraum wall motion and plasma filling. This was overcome by using dynamic beam phasing between the inner and outer cones. Specifically, the inner cone fraction was set high early on the rise to peak power. This allowed drive to reach the equator when a channel was still open, but at the expense of driving a P2 symmetry swing, which in turn generated hydrodynamic jets from the polar regions. This reduced the yield to 10-20% of the 1D value, much lower than the lower convergence symcap. Some improvements can be made by repointing the beams but true 1D implosions require more radical changes to the hohlraum size and shape.

VI. CONCLUSIONS and discussion

HDC ablators have been shown to perform well in ICF implosions using both conventional gas filled and near vacuum hohlraums. Performance in gas filled hohlraums was essentially limited by the hohlraum energetics. HDC produced higher quality implosions than equivalent CH designs. Near vacuum hohlraums have provided an alternate path for higher adiabat implosions with very high velocities and little or no hotspot mix. These high velocities, in excess of the 400km/s required for ignition designs indicate that the hohlraum size can be increased for fixed capsule radius while maintaining adequate drive to achieve ignition velocities. Increasing the case to capsule ratio in this way creates more room for inner beam propagation potentially reducing the need for dynamic beam

phasing. Similarly reshaping the hohlraum near the laser entrance holes can reduce hohlraum wall plasma blow off in the path of the inner beams, improving the drive to the capsule equator. Finally, choosing an intermediate hohlraum gas density should also reduce hohlraum wall plasma filling, further improving inner beam propagation while keeping below thresholds for laser plasma instabilities. A series of 2D simulations indicate that by using all three of these tools, time dependent symmetry should be improved for pulses as long as 9ns, If this can be realized this opens up the possibility of extending the promising near vacuum hohlraums to lower adiabat pulses (such as the 10ns duration 3-shock pulses, $\alpha \sim 2$). A series of experiments are planned to examine this parameter space.

ACKNOWLEDGMENTS

The author would like to acknowledge the efforts of the NIF operations, laser performance, target diagnostics, and target fabrication teams. This work was performed under the auspices of the U.S. Department of Energy by Lawrence Livermore National Laboratory under Contract DE-AC52-07NA27344.

References

1. J. Lindl, P. Amendt, R. Berger, S. Glendinning, S. Glenzer, S. Haan, R. Kauffman, O. Landen, and L. Suter, Physics of Plasmas 11, 339 (2004).
2. E. I. Moses et al. , Phys. Plasmas 16, 041006 (2009).
3. S. W. Haan, J. D. Lindl, D. A. Callahan, D. S. Clark, J. D. Salmonson, B. A. Hammel, L. J. Atherton, R. C. Cook, M. J. Edwards, S. Glenzer, A. V. Hamza, S. P. Hatchett, M. C. Herrmann, D. E. Hinkel, D. D. Ho, H. Huang, O. S. Jones, J. Kline, G. Kyrala, O. L. Landen, B. J. MacGowan, M. M. Marinak, D. D. Meyerhofer, J. L. Milovich, K. A. Moreno, E. I. Moses, D. H. Munro, A. Nikroo, R. E. Olson, K. Peterson, S. M. Pollaine, J. E. Ralph, H. F. Robey, B. K. Spears, P. T. Springer, L. J. Suter, C. A. Thomas, R. P. Town, R. Vesey, S. V. Weber, H. L. Wilkens, and D. C. Wilson, Physics of Plasmas 18, 051001 (2011).
4. Y. Saillard, Nuclear Fusion 46, 1017 (2006).
5. N. B. Meezan, A. J. MacKinnon, D. G. Hicks, E. L. Dewald, R. Tommasini, S. Le Pape, T. Doppner, T. Ma, D. R. Farley, D. H. Kalantar, P. Di Nicola, D. A. Callahan, H. F. Robey, C. A. Thomas, S. T. Prisbrey, O. S. Jones, J. L. Milovich, D. S. Clark, D. C. Eder, M. B. Schneider, K. Widmann, J. A. Koch, J. D. Salmonson, Y. P. Opachich, L. R. Benedetti, S. F. Khan, A. G. MacPhee, S. M. Glenn, D. K. Bradley, E. G. Dzenitis, B. R. Nathan, J. J. Kroll, A. V. Hamza, S. N. Dixit, L. J. Atherton, O. L. Landen, S. H. Glenzer, W. W. Hsing, L. J. Suter, M. J. Edwards, B. J. MacGowan, and E. I. Moses, Phys. Plasmas 20, 056311 (2013).
6. D. G. Hicks, T. R. Boehly, P. M. Celliers, D. K. Bradley, J. H. Eggert, R. S. McWilliams, R. Jeanloz, and G. W. Collins, Phys. Rev. B 78, 174102 (2008).
7. M. D. Knudson, M. P. Desjarlais, D. H. Dolan, Science 322, 1822 (2008).
8. P. M. Celliers, D. J. Erskine, C. M. Sorce, D. G. Braun, O. L. Landen, and G. W. Collins, Rev. Sci. Instrum. 81, 035101 (2010).
9. O. L. Landen, D. K. Bradley, D. G. Braun, V. A. Smalyuk, D. G. Hicks, P. M. Celliers, S. Prisbrey, R. Page, T. R. Boehly, S. W. Haan, D. H. Munro, R. G. Wallace, A. Nikroo, A. Hamza, J. Biener, C. Wild, E. Woerner, R. E. Olson, G. A. Rochau, M. Knudson, D. C.

Wilson, H. F. Robey, G. W. Collins, D. Ho, J. Edwards, M. M. Marinak, B. A. Hammel, D. D. Meyerhofer, and B. J. MacGowan, J. Phys. : Conf. Ser. 112, 022004 (2008).

10. R. P. J. Town, M. D. Rosen, P. A. Michel, L. Divol, J. D. Moody, G. A. Kyrala, M. B. Schneider, J. L. Kline, C. A. Thomas, J. L. Milovich, D. A. Callahan, N. B. Meezan, D. E. Hinkel, E. A. Williams, R. L. Berger, M. J. Edwards, L. J. Suter, S. W. Haan, J. D. Lindl, E. L. Dewald, S. Dixit, S. H. Glenzer, O. L. Landen, E. I. Moses, H. A. Scott, J. A. Harte, and G. B. Zimmerman, Physics of Plasmas 18, 056302 (2011).
11. P. Michel, L. Divol, E. Williams, S. Weber, C. Thomas, D. Callahan, S. Haan, J. Salmonson, S. Dixit, D. Hinkel, M. Edwards, B. MacGowan, J. Lindl, S. Glenzer, and L. Suter, Physical Review Letters 102, 025004 (4 pp.) (2009).
12. P. Michel, S. H. Glenzer, L. Divol, D. K. Bradley, D. Callahan, S. Dixit, S. Glenn, D. Hinkel, R. K. Kirkwood, J. L. Kline, W. L. Kruer, G. A. Kyrala, S. L. Pape, N. B. Meezan, R. Town, K. Widmann, E. A. Williams, B. J. MacGowan, J. Lindl, and L. J. Suter, Physics of Plasmas 17, 056305 (2010).J.
13. Moody et al., Bulletin of Am Phys. Soc 58, 16 (DPP13-2013-001536) and DPP Phys.of Plasmas conf series (2013).
14. M. M. Marinak, G. D. Kerbel, N. A. Gentile, O. Jones, D. Munro, S. Pollaine, T. R. Dittrich, and S. W. Haan, Physics of Plasmas 8, 2275 (2001).
15. M. Rosen, H. Scott, D. Hinkel, E. Williams, D. Callahan, R. Town, L. Divol, P. Michel, W. Kruer, L. Suter, R. London, J. Harte, and G. Zimmerman, High Energy Density Physics 7, 180 (2011).
16. O. S. Jones, C. J. Cerjan, M. M. Marinak, J. L. Milovich, H. F. Robey, P. T. Springer, L. R. Benedetti, D. L. Bleuel, E. J. Bond, D. K. Bradley, D. A. Callahan, J. A. Caggiano, P. M. Celliers, D. S. Clark, S. M. Dixit, T. Doppner, R. J. Dylla-Spears, E. G. Dzentitis, D. R. Farley, S. M. Glenn, S. H. Glenzer, S. W. Haan, B. J. Haid, C. A. Haynam, D. G. Hicks, B. J. Kozioziemski, K. N. LaFortune, O. L. Landen, E. R. Mapoles, A. J. MacKinnon, J. M. McNaney, N. B. Meezan, P. A. Michel, J. D. Moody, M. J. Moran, D. H. Munro, M. V. Patel, T. G. Parham, J. D. Sater, S. M. Sepke, B. K. Spears, R. P. J. Town, S. V. Weber, K. Widmann, C. C. Widmayer, E. A. Williams, L. J. Atherton, M. J. Edwards, J. D. Lindl, B. J. MacGowan, L. J. Suter, R. E. Olson, H. W. Herrmann, J. L. Kline, G. A.

Kyrala, D. C. Wilson, J. Frenje, T. R. Boehly, V. Glebov, J. P. Knauer, A. Nikroo, H. Wilkens, and J. D. Kilkenny, Physics of Plasmas 19, 056315 (2012).

17. M.M. Biener, J. Biener, S.O. Kucheyev, Y.M. Wang, B. El-Dasher, N.E. Teslich, A.V. Hamza, H. Obloh, W. Mueller-Sebert, M. Wolfer, T. Fuchs, M. Grimm, A. Kriele, C. Wild, Diamond & Related Materials **19** 643–647 (2010).
18. Ma, T.; Patel, P. K.; Izumi, N.; et al. Phys. Rev. Lett. 111 085004 (2013)
19. C. Cerjan, P. Springer, S. Sepke Physics of Plasmas 20, 056319 (2013).
20. J. L. Kline, S. H. Glenzer, R. E. Olson, L. J. Suter, K. Widmann, D. A. Callahan, S. N. Dixit, C. A. Thomas, D. E. Hinkel, E. A. Williams, et al., Physical Review Lett. 106, 085003 (2011); S. LePape et al., submitted to Phys. Rev. Lett. (2013).
21. J. D. Moody, P. Datte, K. Krauter et al., Rev. Sci. Instrum. 81, 6 (2010).
22. E. L. Dewald, C. Thomas, S. Hunter et al., Rev. Sci. Instrum. 81, 3 (2010).
23. R. L. Kauffman, H. N. Kornblum, D. W. Phillion et al., Rev. Sci. Instrum. **66**, 678 (1995).
24. H. N. Kornblum, R. L. Kauffman, and J. A. Smith, Rev. Sci. Instrum. **57**, 2179 (1986).
25. E. L. Dewald, K. M. Campbell, R. E. Turner et al., Rev. Sci. Instrum. **75** (2004).
26. J. L. Kline, K. Widmann, A. Warrick et al., Review of Scientific Instruments **81** (2012).
27. G. A. Kyrala, S. Dixit, S. Glenzer, D. Kalantar, D. Bradley, N. Meezan Izumi, N. O. L. Landen, D. Callahan, S. V. Weber, J. P. Holder, S. Glenn, M. J. Edwards, P. Bell, J. Kimbrough, J. Koch, R. Prasad, L. Suter, J. L. Kline, and J. Kilkenny, Rev. Sci. Instrum. 81, 10E316 (2010).
28. D. G. Hicks, N. B. Meezan, E. L. Dewald, A. J. Mackinnon, D. A. Callahan, T. Doeppner, L. R. Benedetti, D. K. Bradley, P. M. Celliers, D. S. Clark, S. N. Dixit, E. G. Dzenitis, J. E. Eggert, D. R. Farley, S. M. Glenn, S. H. Glenzer, A. V. Hamza, R. F. Heeter, J. P. Holder, N. Izumi, D. H. Kalantar, S. F. Khan, J. J. Kroll, T. Ma, A. G. MacPhee, J. M. McNaney, J. D. Moody, M. J. Moran, B. R. Nathan, K. P. Opachich, R. R. Prasad, J. E. Ralph, H. F. Robey, J. R. Rygg, J. D. Salmonson, M. B. Schneider, N. Simanovskaia, B. K. Spears, R. Tommasini, K. Widmann, G. W. Collins, O. L. Landen, J. D. Kilkenny, W. W. Hsing, B. J.MacGowan, L. J. Atherton, M. J. Edwards, R. E. Olson, J.

A. Frenje, R. D. Petrasso, H. G. Rinderknecht, A. B. Zylstra, J. L. Kline, G. A. Kyrala, and A. Nikroo, Phys. Plasmas 19, 122702 (2012).

29. R.Rygg submitted to Phys. Rev. Lett. (2013).

30. VISAR L. M. Barker and R. E. Hollenbach, J. Appl. Phys. 43, 4669 (1972);

31. P. M. Celliers, D.K. Bradley, G. W. Collins, D. G. Hicks, T. R. Boehly, and W. J. Armstrong, Rev. Sci. Instrum. 75, 4916 (2004).

32. H. F. Robey, T. R. Boehly, P. M. Celliers, J. H. Eggert, D. Hicks, R. F. Smith, R. Collins, M. W. Bowers, K. G. Krauter, P. S. Datte, D. H. Munro, J. L. Milovich, O. S. Jones, P. A. Michel, C. A. Thomas, R. E. Olson, S. Pollaine, R. P. J. Town, S. Haan, D. Callahan, D. Clark, J. Edwards, J. L. Kline, S. Dixit, M. B. Schneider, E. L. Dewald, K. Widmann, J. D. Moody, T. D¨oppner, H. B. Radousky, A. Throop, D. Kalantar, P. DiNicola, A. Nikroo, J. J. Kroll, A. V. Hamza, J. B. Horner, S. D. Bhandarkar, E. Dzenitis, E. Alger, E. Giraldez, C. Castro, K. Moreno, C. Haynam, K. N. LaFortune, C. Widmayer, M. Shaw, K. Jancaitis, T. Parham, D. M. Holunga, C. F. Walters, B. Haid, E. R. Mapoles, J. Sater, C. R. Gibson, T. Mals- bury, J. Fair, D. Trummer, K. R. Co□ee, B. Burr, L. V. Berzins, C. Choate, S. J. Brereton, S. Azevedo, H. Chandrasekaran, D. C. Eder, N. D. Masters, A. C. Fisher, P. A. Sterne, B. K. Young, O. L. Landen, B. M. Van Wonterghem, B. J. MacGowan, J. Atherton, J. D. Lindl, D. D. Meyerhofer, and E. Moses, Physics Of Plasmas 19, 042706 (2012).

33. J. Frenje et al., Nucl. Fusion 53 (2013) 043014 (2013)

34. Edgell, D. H.; Bradley, D. K.; Bond, E. J.; et al. Rev. Sci Instrumen 83m 10E119 (2012)

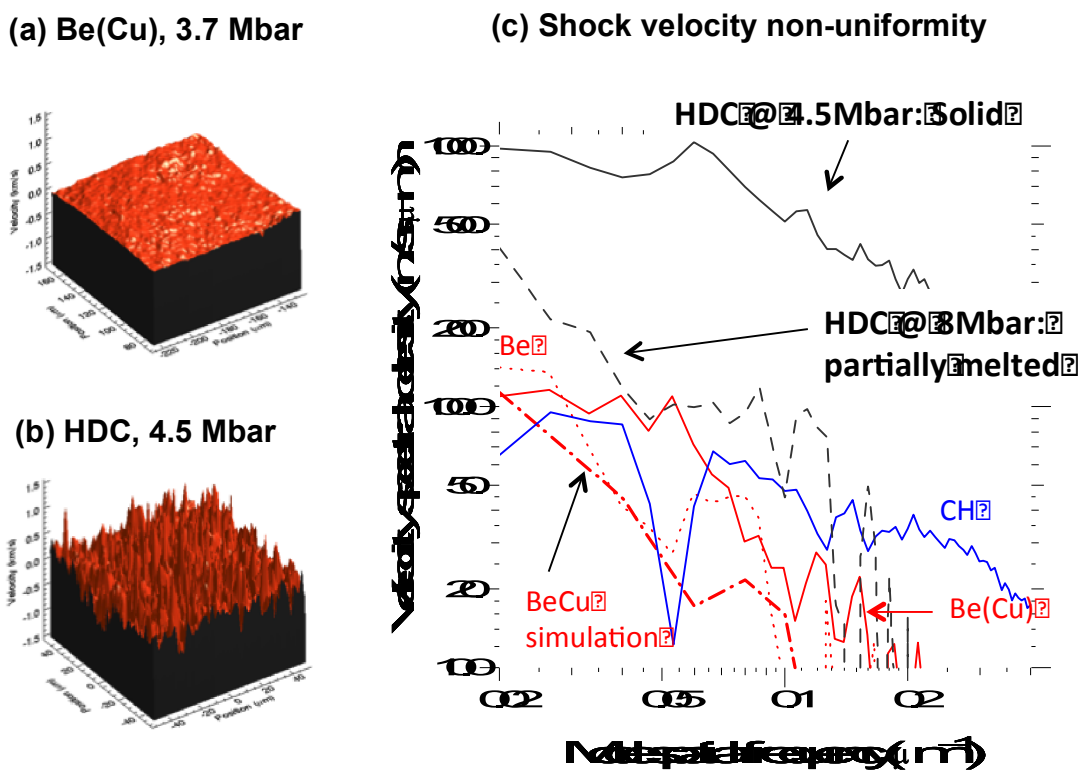

Figure 1: Experimental results from experiments on the Omega facility showing shock uniformity vs shock strength for (a) Be and (b) HDC (c) HDC for 4.5 and 8Mbar shocks vs CH, Be and Be(Cu) copper doped berylium.

Parameter	HDC ablator designs			CH ablator [3]
No of shocks	2	3	4	4
Fuel Adiabat	3.7	2.0	1.5	1.4
Dopant	undoped	0.25% W	0.25% W	2% Si
HI Growth factor*	180	2000	4000	2500
V_{fuel} (km/s)	380	383	380	370
1D yield(MJ)	0.05	17	20	11
ρR_{fuel} (gcm^{-2})	0.9	1.25	1.42	1.6

* Peak ablation front growth factor [3]

Table.1 summary of 1D performance and growth factors for HDC and CH designs

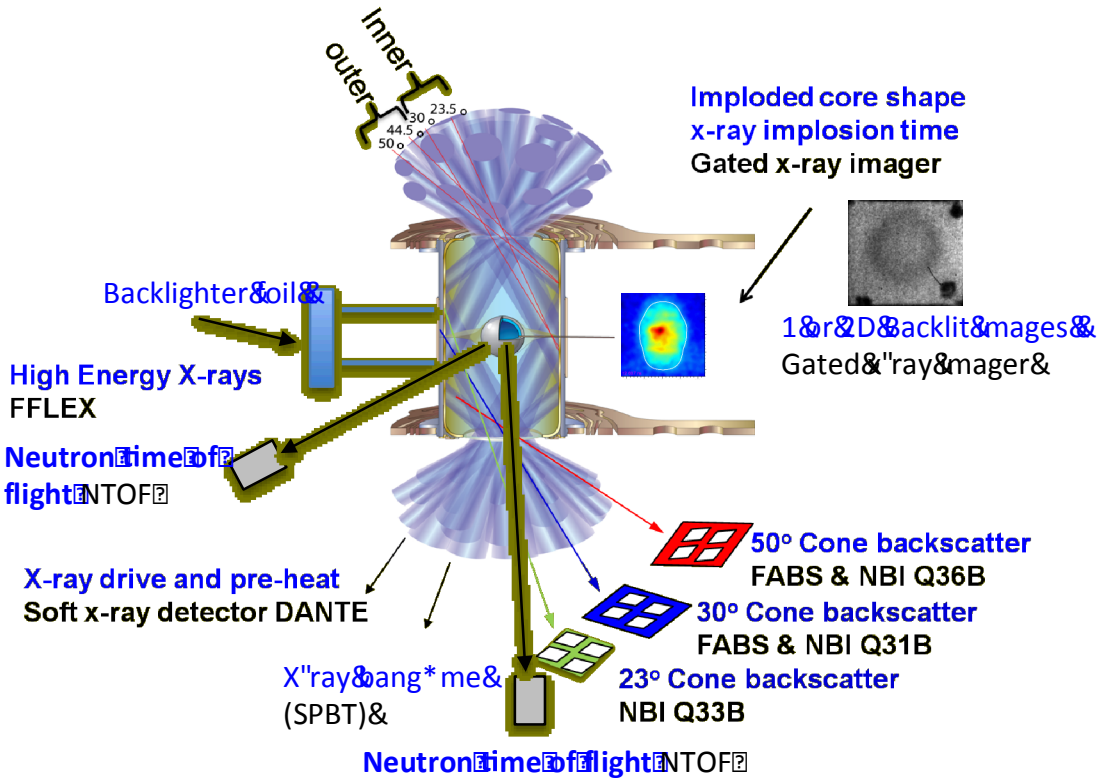

Figure 2: Experimental setup for gold hohlraums including the equatorial x-ray self-emission, backlit images, neutron time of flight detectors and south pole bangtime detector.

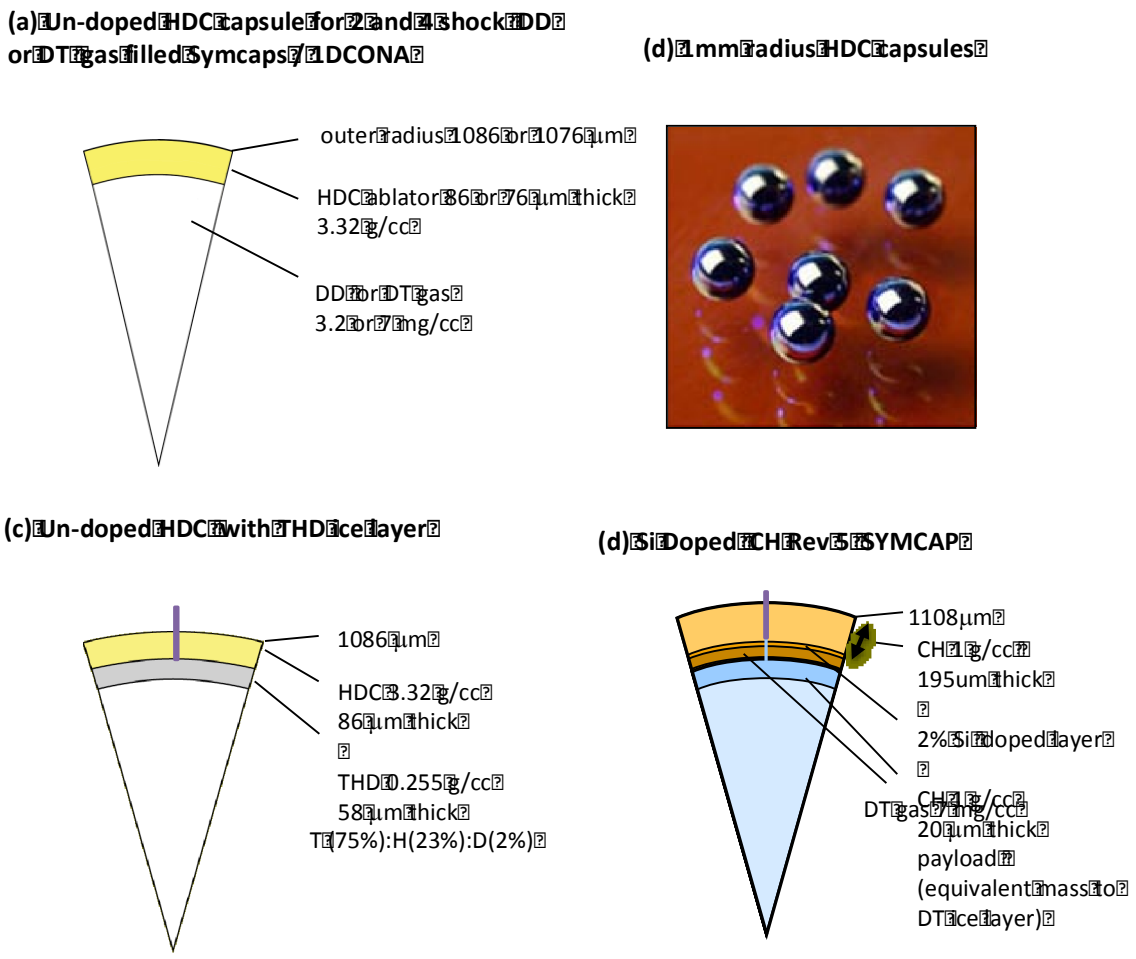

Figure.3 (a) Undoped HDC capsule with either 76um (4-shock experiments) or 86 um (2-shock experiments) thick ablators (b) Silicon doped CH capsule used for CH DT filled symcap experiments and (c) undoped HDC ablator with THD ice layer used for the THD 2DCONA experiments

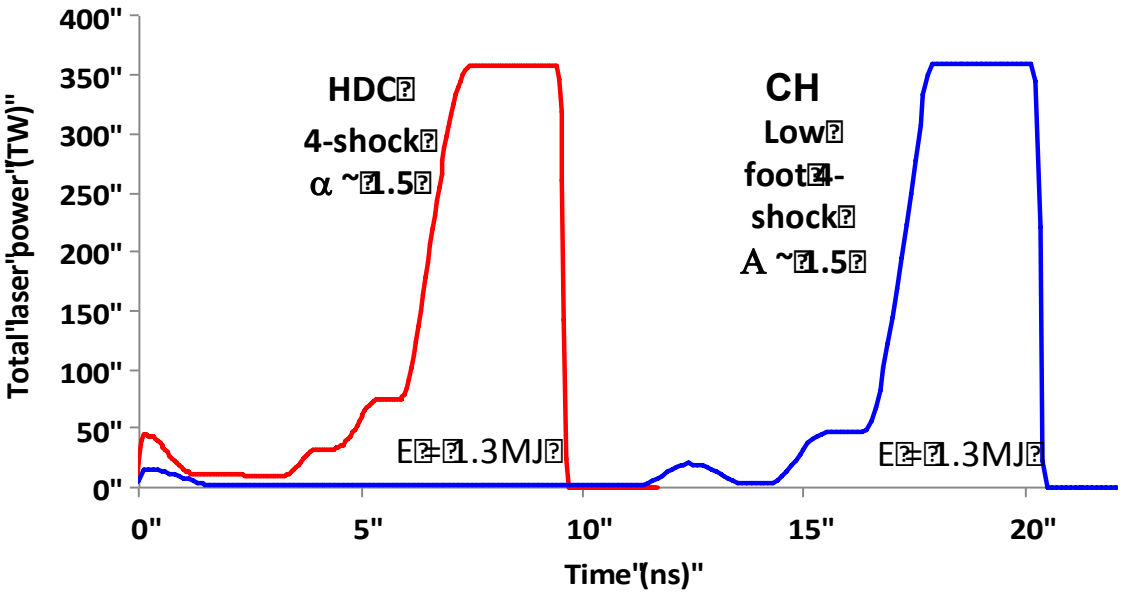

Figure 4: The requested laser pulse shape for HDC (red line) is compared to the Low-foot CH pulse (blue line). Both laser pulses have a total energy of 1.3 MJ and powers between 350 and 360 TW.

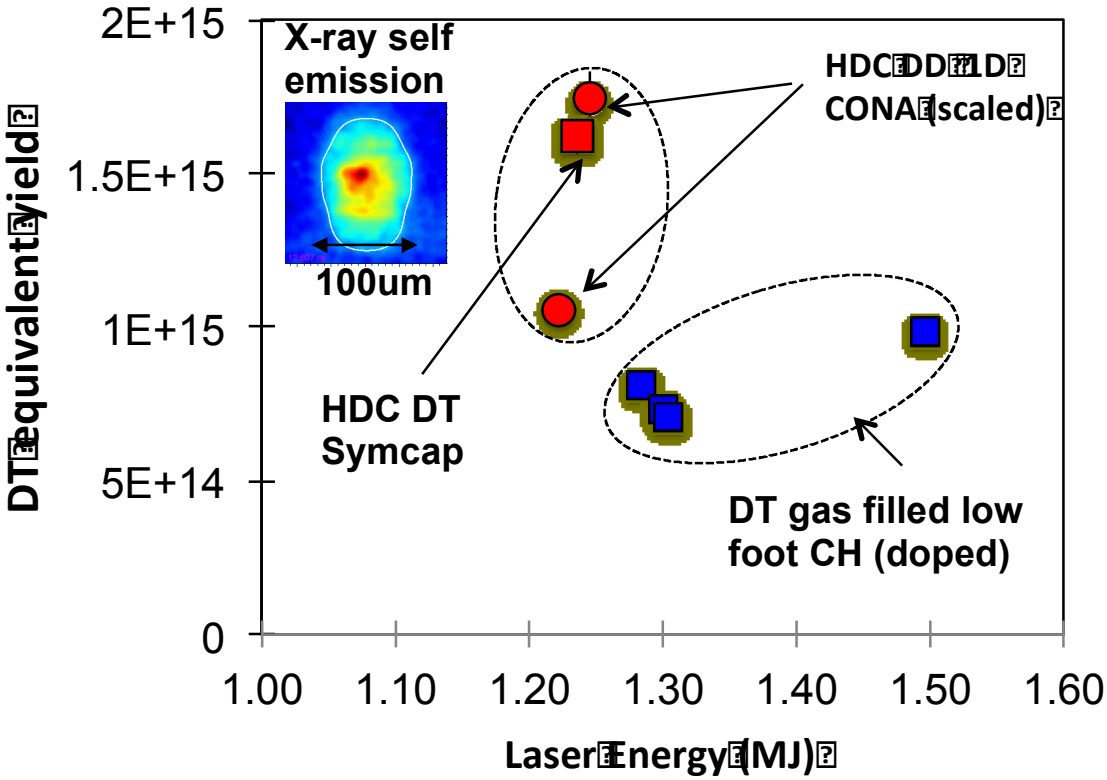

Fig.5: DT equivalent yield vs laser drive energy for gas filled HDC and CH 4-shock implosions driven by gas filled hohlraums. Two DD HDC implosions are included by scaling their measured DD neutron yield by a factor of 100 to account for the difference in DT vs DD cross section at ion temperatures ~2.5- 3.0keV. Inset in top left corner shows gated x-ray image at stagnation from the HDC DT symcap

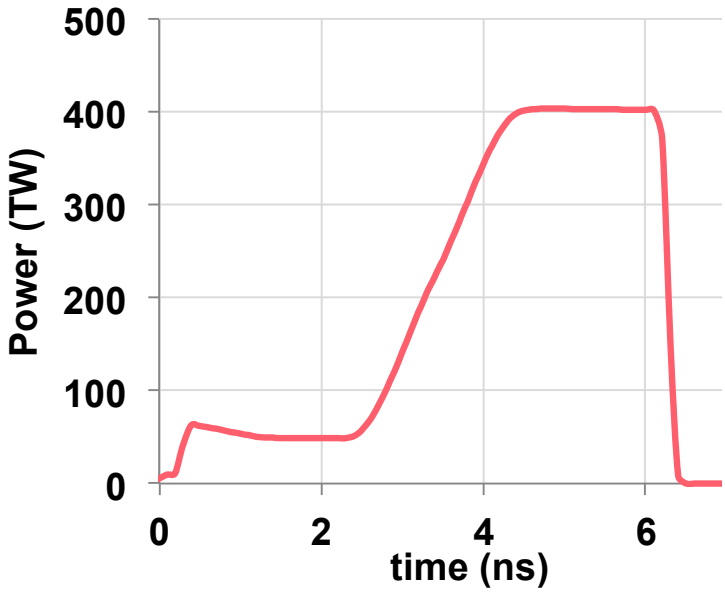

Fig. 6: 2-shock laser pulseshape for driving a symcap in a near vacuum hohlraum with 86um thick undoped HDC ablator. The laser energy was 1.3MJ with peak power of 400TW.

Parameter	*Postshot drive	Expt
Mband fraction (>1.8 keV)	22%	22%
Yield (DD)	2.4e13	2.3e13
T_{ion} (keV)	3.3	3.4
Laser – Hohl. coupling	N/A	98%
Bang time (ns)	7.75	7.77
P0 (μm)	101	91
Velocity (km/s)	430	N/A

* drive adjusted for delivered energy and observed spectrum

Table 2. Comparison of post-shot calculated vs measured implosion performance for a DD filled HDC target driven by a NVH with a 2-shock pulsehape.

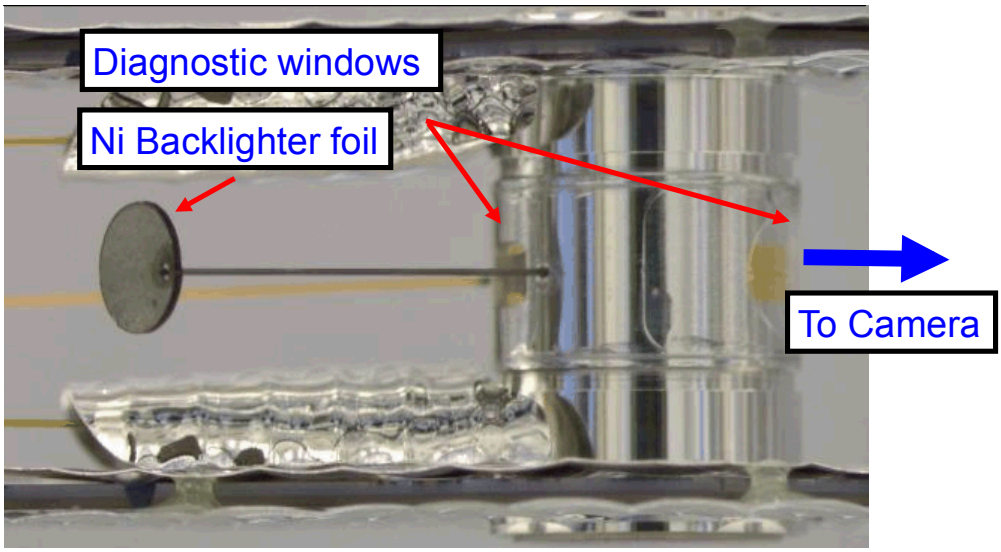

Fig. 7: 2DCONA target showing hohlraum with Ni backlighter foil and diagnostic windows.

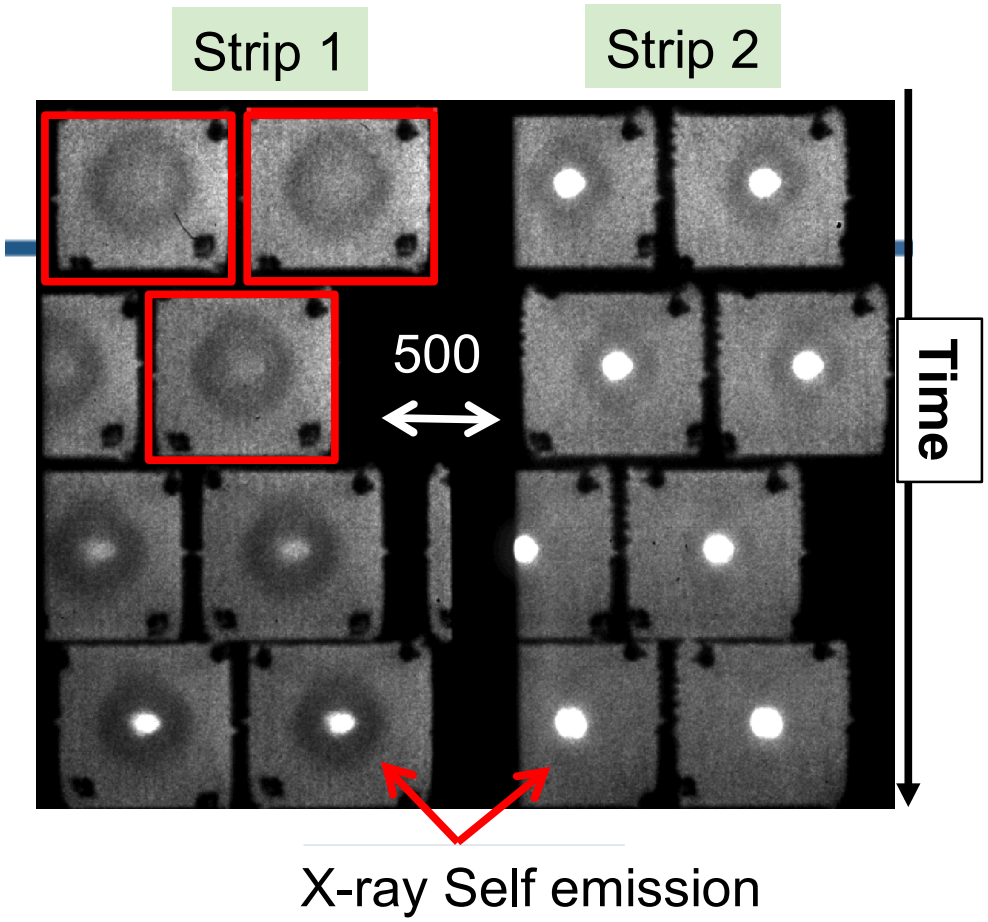

Figure 8: 2D radiography data using 7.8keV x-rays backlighting the imploding HDC capsule at 350ps to 100ps before bang time.

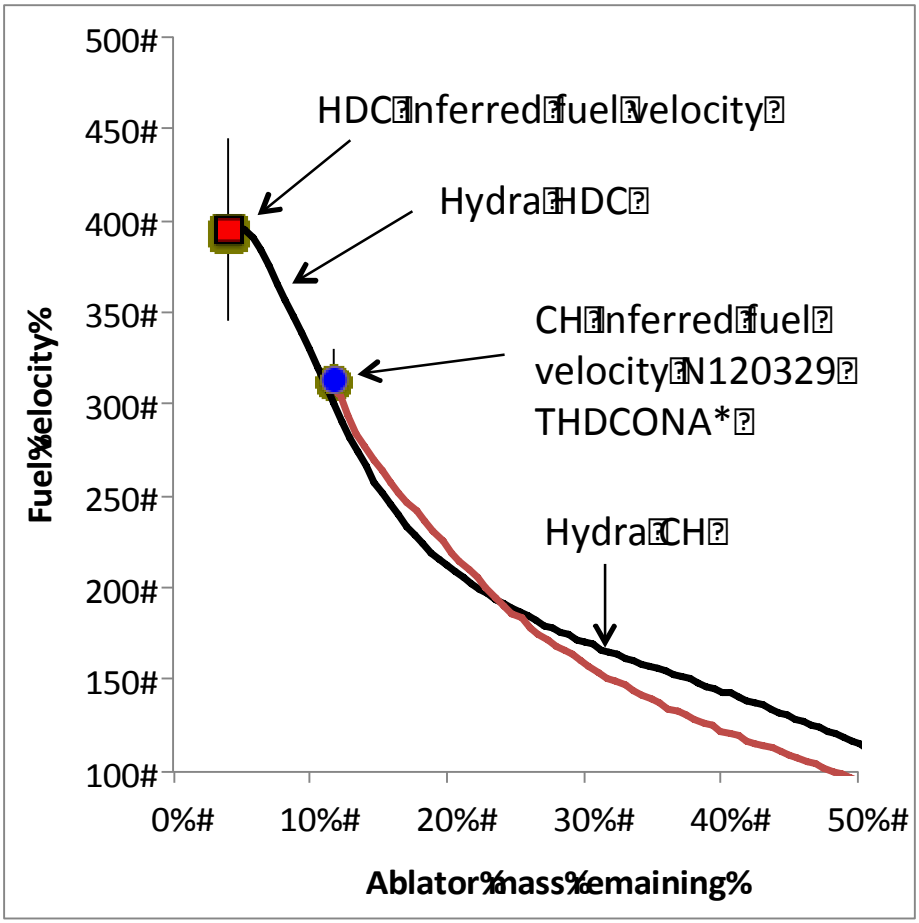

Figure 9: Inferred fuel velocity vs Ablator mass remaining for HDC NVH and equivalent CH implosion experiment from a gas filled holraum. Also shown are Hydra post-shot simulations for these implosions

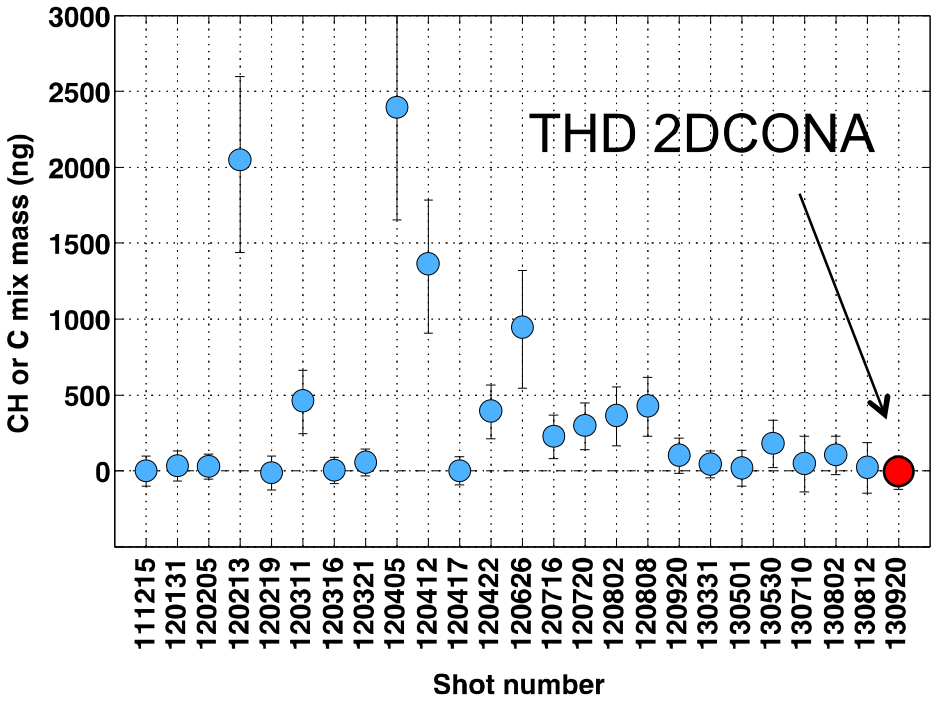

Figure 10: Plot of inferred ng of CH or C mass mixed into the hotspot as a function of shot number for a series of CH implosions and the THD 2DCONA using the HDC ablator.